

The Effect of Carbon Additions on the Creep Resistance of Fe-25Al-5Zr Alloy



FERDINAND DOBEŠ, VĚRA VODIČKOVÁ, JOZEF VESELÝ,
and PETR KRATOCHVÍL

Creep experiments were conducted on Fe-25 at. pct Al-5 at. pct Zr alloy with carbon additions at the temperatures of 973 K and 1173 K (700 °C and 900 °C). The alloys were tested in two different states: (i) cast and (ii) annealed at 1273 K (1000 °C) for 50 hours. Stress exponents and activation energies were estimated. The values of the stress exponent n could be explained by the dislocation motion controlled by climb. The increased values of n in the high-carbon alloy at the temperature of 1173 K (900 °C) can be described by means of the threshold stress concept. The creep resistance at 973 K (700 °C) decreased with the increasing content of carbon. This result is discussed in terms of the ratio of zirconium to carbon in the alloy. An increase of the creep resistance with increasing ratio Zr:C is in agreement with the behavior observed previously in alloys with substantially lower concentrations of zirconium.

DOI: 10.1007/s11661-016-3770-6

© The Minerals, Metals & Materials Society and ASM International 2016

I. INTRODUCTION

THE intermetallic alloys based on the compounds Fe₃Al and FeAl are prospective candidates for high-temperature structural applications.^[1–3] Alloying by refractory metals continues to be the most attractive way toward improvement of their mechanical properties.^[4–11] Several methods can be adopted to enhance limited creep resistance: these consist mainly of adding elements for either solid solution strengthening or precipitation strengthening.^[12,13] The precipitation strengthening is determined by the low solubility of the added elements. From this point of view, the alloying by zirconium may be of interest because nearly no solid solubility for Zr exists in the Fe-Al phases. The beneficial effect of zirconium addition on creep resistance was first reported for the Fe-28 pct Al-based alloy (at. pct is given throughout) by McKamey *et al.*^[14–16] and the Fe-40 pct Al-based alloy by Whittenberger *et al.*^[17] Moreover, a positive effect of a dispersion of fine Zr-rich carbides was demonstrated *via* microstructural analysis.^[14] Subsequent studies focused on the additions of various amounts of zirconium to a wide range of Fe-Al alloys.^[18–24] Less attention has been devoted to the combined additions of zirconium and carbon. The results of these studies are summarized elsewhere.^[25] Carbon content appears to be

beneficial in suppressing the hydrogen embrittlement at grain boundaries.^[26]

The effect of the additives Zr (0.2 to 0.3 pct) and C (0.2 to 0.6 pct) on the phase composition and high-temperature mechanical properties of Fe₃Al-type alloys was investigated in our previous paper.^[25] It was shown that the ratio of zirconium to carbon additives influenced the phase structure and played an important role in determining the mechanical properties. The purpose of the present paper is to examine the influence of larger carbon additions (up to 3.5 pct) on the compressive creep of Fe-25Al alloy with similarly increased zirconium content (5 pct).

II. EXPERIMENTAL

The examined alloys were prepared by vacuum melting and casting; Zr was added in metallic form. The dimensions of the cast ingot of the low-carbon alloy were 20 × 40 × 150 mm³. The casts of alloys with added carbon measured 10 × 15 × 30 mm³. The chemical compositions are listed in Table I.

Some samples were additionally annealed at 1273 K (1000 °C) for 50 hours in sealed ampoules that were filled with helium to stabilize the microstructure prior to the creep tests. The annealing was followed by rapid cooling in air outside the furnace. These samples are denoted as “annealed.” The microstructures were studied using a Zeiss Ultra Plus field emission scanning electron microscope (SEM) equipped with both an OXFORD X-MAX 20 energy-dispersive spectrometer and an OXFORD NordlysNano detector for electron backscatter diffraction (BSE). Transmission electron microscopy (TEM) was done on JEOL JEM-2000FX at 200kV. Samples were prepared by electropolishing in 20 pct HNO₃ in methanol at 243 K (–30 °C) and 15 V.

FERDINAND DOBEŠ, Senior Researcher, is with the Institute of Physics of Materials, Academy of Sciences of the Czech Republic, Žitkova 22, 616 62 Brno, Czech Republic. Contact e-mail: dobes@ipm.cz VĚRA VODIČKOVÁ, Senior Assistant Professor, is with the Department of Material Science, Faculty of Mechanical Engineering, Technical University of Liberec, Hálkova 6, 461 17 Liberec 1, Czech Republic. JOZEF VESELÝ, Junior Researcher, and PETR KRATOCHVÍL, Professor, are with the Department of Physics of Materials, Faculty of Mathematics and Physics, Charles University in Prague, Ke Karlovu 5, 121 16 Prague 2, Czech Republic.

Manuscript submitted March 24, 2016.

Article published online September 21, 2016

Table I. Composition of the Alloys (At. Pct)

Alloy	Al	Zr	C
Fe-25Al-5Zr	25.4	5.0	0.06
Fe-25Al-5Zr-1C	25.3	5.65	0.92
Fe-25Al-5Zr-4C	24.7	5.42	3.46

The creep tests were performed in uniaxial compression on samples with a gage length of 12 mm and a cross-section of $5 \times 5 \text{ mm}^2$ (low-carbon alloy) or a gage length of 6.5 mm and a cross-section of $3 \times 3 \text{ mm}^2$ (two high-carbon alloys). The samples were prepared by traveling wire electro-discharge machining and fine grinding of the surfaces. The tests were performed under a constant load in a protective atmosphere of dry purified argon at temperatures of 973 K and 1173 K (700 °C and 900 °C). Changes in specimen length were measured using a linear variable displacement transducer. The samples were subjected to stepwise loading, where the load was changed after the steady-state creep rate was established for a given load. The terminal values of the true stress and the creep rate, *i.e.*, the true compressive strain rate, were evaluated for each step.

III. RESULTS

A. Microstructure

1. Fe-25Al-5Zr

The microstructure of this alloy is documented in the previous paper.^[27] In agreement with the available ternary diagram,^[28] the microstructure consists of primary solidified bcc α (disordered solid solution of Al in Fe, body-centered cubic A2 lattice) surrounded by a eutectic composed of alternating lamellae of α and λ_1 Laves phase $(\text{Fe,Al})_2\text{Zr}$. The bcc lattice α changes as the temperature decreases, becoming an ordered B2 lattice at 1026 K (753 °C) and an ordered D0₃ lattice at temperatures below 815 K (542 °C).^[29] The volume fraction of the eutectic is equal to 47.6 pct. ZrC particles with a diameter of $\sim 2 \mu\text{m}$ are also present in the alloy. These particles were formed due to the presence of a small amount of carbon as an impurity in the iron used for casting. The volume fraction of ZrC does not exceed 0.02 pct.

The heat treatment of this alloy, as well as all alloys studied in the present paper, caused coagulation of the eutectic lamellae of λ_1 Laves phase; the microstructure is composed of a matrix α with λ_1 particles. The volume fraction of λ_1 is 27.7 pct. The small ZrC particles remain, even after the heat treatment, and are wrapped in the λ_1 phase.

2. Fe-25Al-5Zr-1C

The microstructure of the cast Fe-25Al-5Zr-1C alloy is again characterized by the presence of primary solidified α and the eutectic composed of α and λ_1 Laves phase $(\text{Fe,Al})_2\text{Zr}$. ZrC particles (*e.g.*, plates or dendritic formations, size 3 to 10 μm) are also present in the alloy (Figure 1).

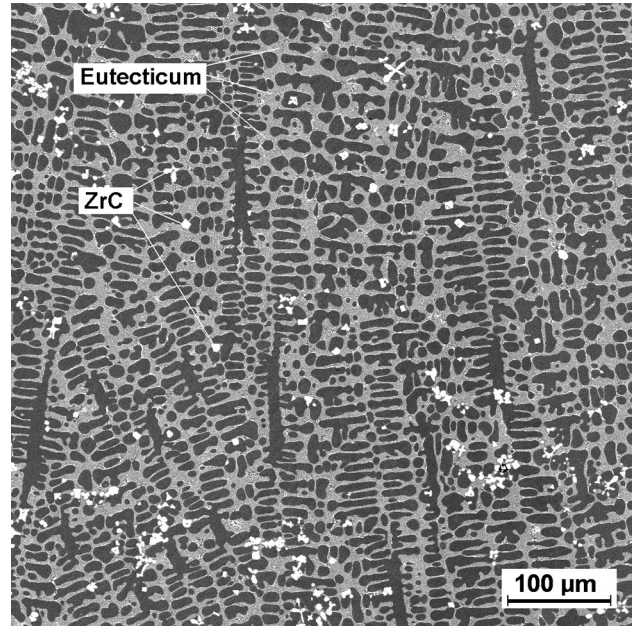


Fig. 1—Back-scattered electron (BSE) image of the microstructure in the cast Fe-25Al-5Zr-1C alloy. The matrix α is the dark phase, the eutectic $\lambda_1 + \alpha$ is gray, and the small bright particles are ZrC.

Table II. Summary of Fractions (Vol Pct) of Observed Phases in the Studied Alloys

	0.06 At. Pct C	0.92 At. Pct C	3.46 At. Pct C
Cast			
Eutecticum	47.6	40.9	12.2
ZrC	≤ 0.02	1.8	6.2
Annealed			
Laves phase	27.7	21.3	5.9*
ZrC	≤ 0.02	0.2	4.8

* The value is very little enhanced by the tiny particles of $\text{Fe}_{23}\text{Zr}_6$, which are seen in the picture.

Coagulated Laves phase and small remnants of the eutectic are present in the microstructure of the alloy after heat treatment. A small amount of ZrC phase remains inside the coagulated Laves phase particles (Figure 2). The volume fractions of eutectic and ZrC in cast alloy and of Laves phase and ZrC in annealed alloy, respectively, are listed in Table II. TEM enables to observe small particles (size 0.5 to 1 μm) identified by SAED (selected area electron diffraction) as $\text{Fe}_{23}\text{Zr}_6$ phase (fcc structure of the $\text{Mn}_{23}\text{Th}_6$ type, lattice parameter 1.18 nm), see the microstructure after creep tests, Section III-B. These particles correspond to the metastable phase identified previously in Fe-Al-Zr ternary alloys and stabilized by impurities.^[28]

3. Fe-25Al-5Zr-4C

The square-shaped ZrC particles (sizes from 1 to 15 μm) and eutectic composed α and λ_1 Laves phase $(\text{Fe,Al})_2\text{Zr}$ are present in the microstructure of the cast alloy Fe-25Al-5Zr-4C (Figure 3). The volume fraction of eutectic is markedly lower than that in the

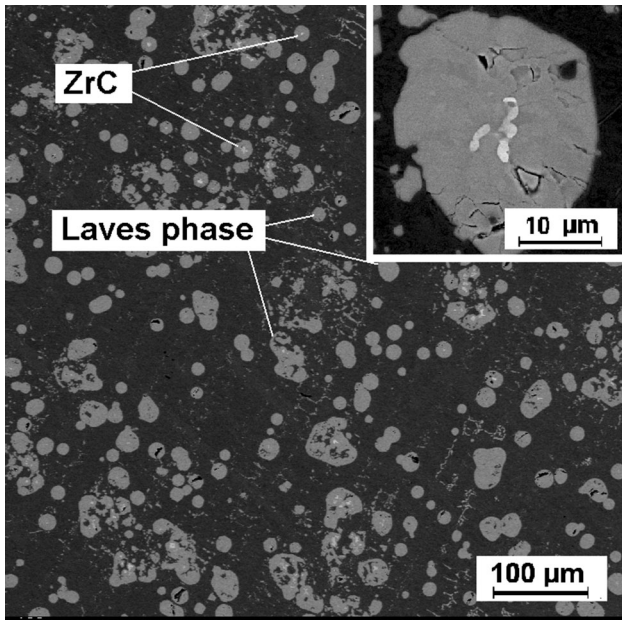


Fig. 2—BSE image of the microstructure in the annealed Fe-25Al-5Zr-1C alloy composed of three phases: α matrix (dark), λ_1 particles (mostly oval-gray), and ZrC particles as bright cores inside λ_1 particles (detail is shown in inset). The smallest particles of $\text{Fe}_{23}\text{Zr}_6$ are visible as gray spots.

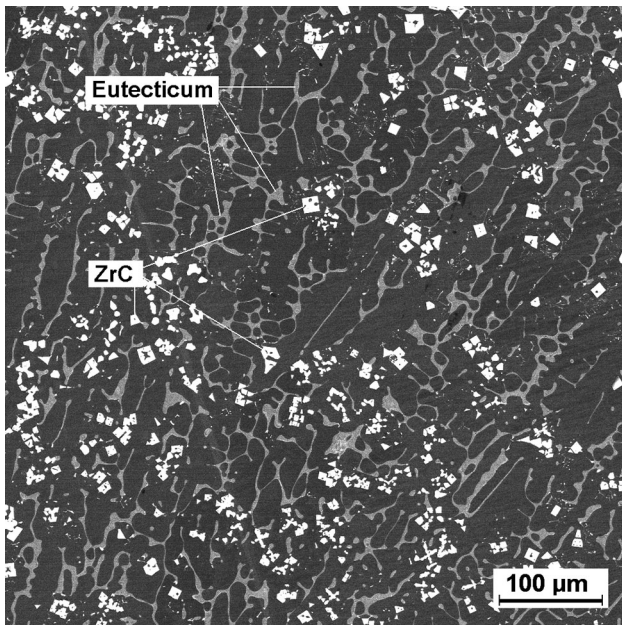


Fig. 3—BSE image of the microstructure in the cast Fe-25Al-5Zr-4C alloy. The matrix α is the dark phase, the eutectic $\lambda_1 + \alpha$ is gray, and the small bright particles are ZrC.

Fe-25Al-5Zr-1C alloy. The microstructure of the annealed alloy is characterized by the presence of “chain-like” particles of Laves phase and square-shaped ZrC carbides (Figure 4). The volume fractions are listed in Table II. The volume fraction of the metastable phase $\text{Fe}_{23}\text{Zr}_6$ was not measurable.

Table III. Activation Energies Q Found by Multiple Regressions Under the Assumption of Temperature-Independent Stress Exponents

	0.06 At. Pct C	0.92 At. Pct C	3.46 At. Pct C
Cast			
Q (kJ/mole)	460	452	415
n , 973 K (700 °C)	6.1	7.0	7.3
r^2	0.945	0.973	0.966
n , 1173 K (900 °C)	7.2	5.7	13.5
r^2	0.991	0.921	0.966
Annealed			
Q (kJ/mole)	362	257	204
n , 973 K (700 °C)	5.8	6.6	6.9
r^2	0.994	0.970	0.998
n , 1173 K (900 °C)	5.7	7.2	9.6
r^2	0.952	0.739	0.991

Stress exponents n and the corresponding correlation coefficients r^2 are calculated separately for each test temperature.

B. Creep

Figure 5 shows the microstructure of the annealed Fe-25Al-5Zr-1C alloy after creep at 1173 K (900 °C) for 382 hours. Dislocations are anchored at particles of $\text{Fe}_{23}\text{Zr}_6$. Dislocations with same particles $\text{Fe}_{23}\text{Zr}_6$ in alloy Fe-25Al-5Zr-4C after creep at 973 K (700 °C) for 315 hours are shown in Figure 6.

The dependence of the creep rate $\dot{\epsilon}$ on the applied stress σ at the various temperatures is shown in Figures 7(a) through (c) on a double logarithmic scale for both cast and annealed states. The data were analyzed using the following relation:^[30]

$$\dot{\epsilon} = A\sigma^n \exp\left(\frac{Q}{RT}\right), \quad [1]$$

where A is a material constant, n is the stress exponent, Q is the activation energy for creep, R is the gas constant, and T is the absolute temperature. The values of Q were estimated from Eq. [1] by multiple linear regression, assuming that the activation energy is independent of stress. The stress exponent n was calculated separately for each test temperature. Correlation coefficients r^2 of these calculations are also given. The obtained values for all investigated alloys are summarized in Table III.

IV. DISCUSSION

The estimated activation energies for creep of cast alloys are higher than the values reported for the Fe-Al alloys with a similar aluminum content (302 to 418 kJ/mol).^[2,31] The energy of 460 kJ/mol for the cast low-carbon alloy is in good agreement with that for the alloys with aluminum contents between 39.8 and 48.7 pct.^[32,33] In any case, all activation energies found in cast alloys are considerably higher than the activation enthalpy for diffusion of both the Fe and Al in Fe-25 at. pct Al, with values of 217 kJ/mol (Fe in A2 lattice), 232 kJ/mol (Fe in B2 lattice),^[34] and 267.1 kJ/mol (Al in

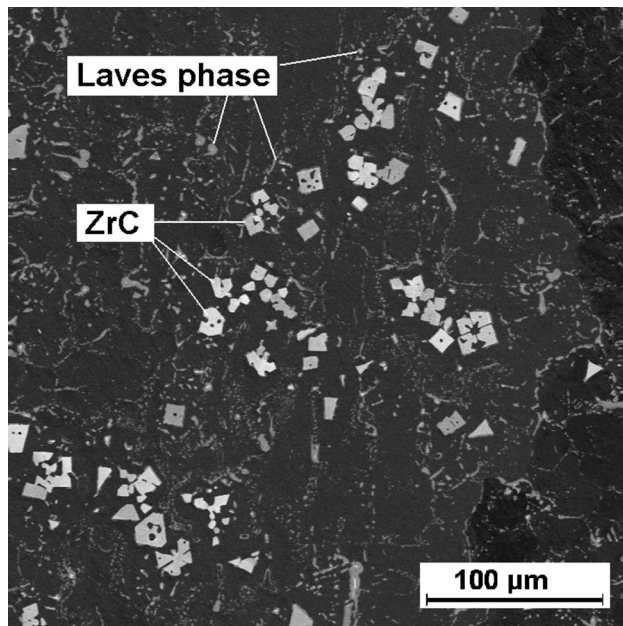


Fig. 4—BSE image of the microstructure in the annealed Fe-25Al-5Zr-4C alloy composed of three phases: α matrix (dark), λ_1 particles (gray), and square shape ZrC particles (bright).

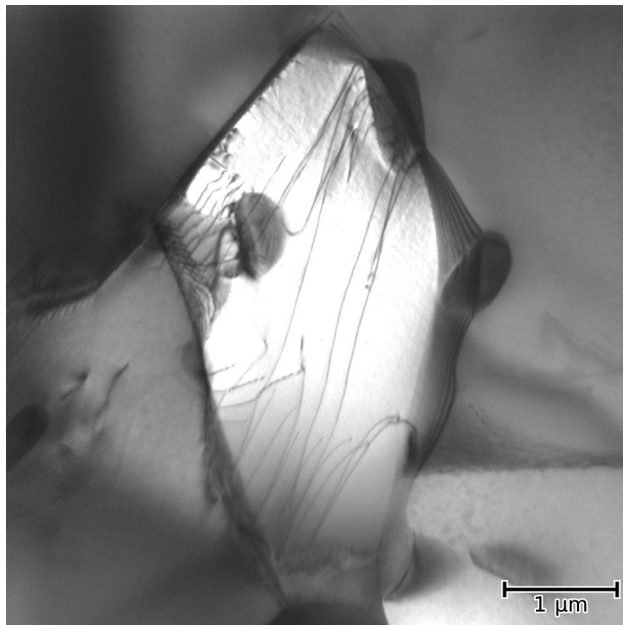


Fig. 5—Interaction of dislocations with particles of $\text{Fe}_{23}\text{Zr}_6$ in the alloy Fe-25Al-5Zr-1C after creep at 1173 K (900 °C).

A2 lattice).^[35] The reasons for this discrepancy can be found in the changing microstructure of the cast alloys at the testing temperature of 1173 K (900 °C). This assumption is supported by comparison of the creep rates of cast and the annealed states: The annealing increases the creep rate at 973 K (700 °C) but has only a limited effect on creep at 1173 K (900 °C): The holding

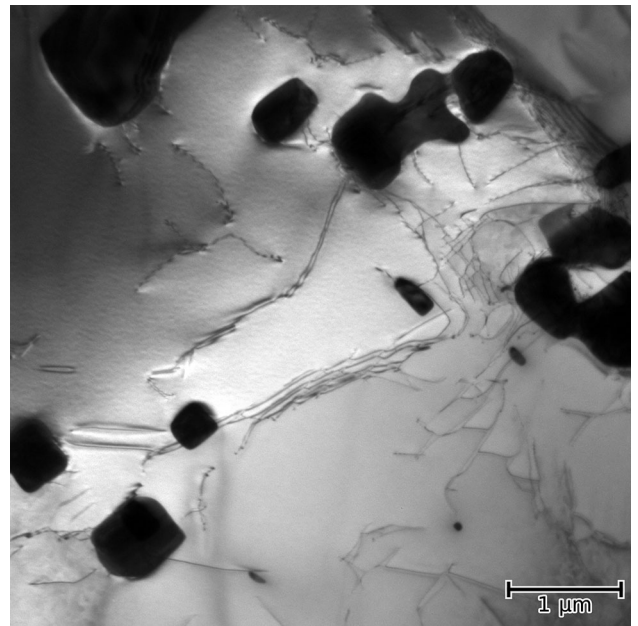


Fig. 6—Example of observation of dislocations and particles $\text{Fe}_{23}\text{Zr}_6$ in the alloy Fe-25Al-5Zr-4C after creep at 973 K (700 °C).

time at the temperature of 1173 K (900 °C) prior to the first reading of the creep rate was longer than 45 hours and sufficiently long such that the eutectic microstructure in cast alloys could coagulate and form an appearance close to that observed after annealing at 1273 K (1000 °C). The estimated activation energy for creep in the annealed alloy can thus be considered appropriate for a phenomenological description of creep data from the viewpoint of microstructural stability. The exact analysis of the activation energy derived experimentally from Eq. [1] is complicated by the changes in the crystal lattice of the matrix. The presence of carbon increases transformation temperature from ordered B2 lattice to disordered A2 lattice [*i.e.*, 1026 K (753 °C)] by approximately $\Delta T = 40$ K (40 °C) due to the addition of 0.5 to 1.0 at. pct C.^[36] Different lattices can be expected in creep experiments at different temperatures. Strict interpretation of the activation energy depends also on the identity of deformation processes at different temperatures. This is not guaranteed due to an excessive difference in applied stresses. The estimated activation energies are only apparent values.

The heterogeneous nature of the present alloys suggests that their behavior can be interpreted in terms of the composite model of deformation.^[37] The local stresses are redistributed to lower values in the “soft” Fe-Al matrix and to higher values in the “hard” Laves phase particles. The estimated activation energy reflects contributions from both phases. (The deformation of carbide ZrC is not probable due to its high melting point and high activation energy of creep, ~ 700 kJ/mol).^[38] The observed decrease in the activation energy with the increasing carbon content can thus be connected to a lower amount of the Laves phase (unfortunately, diffusion data for the $(\text{Fe,Al})_2\text{Zr}$ Laves phase are not available). The estimated values must be taken with

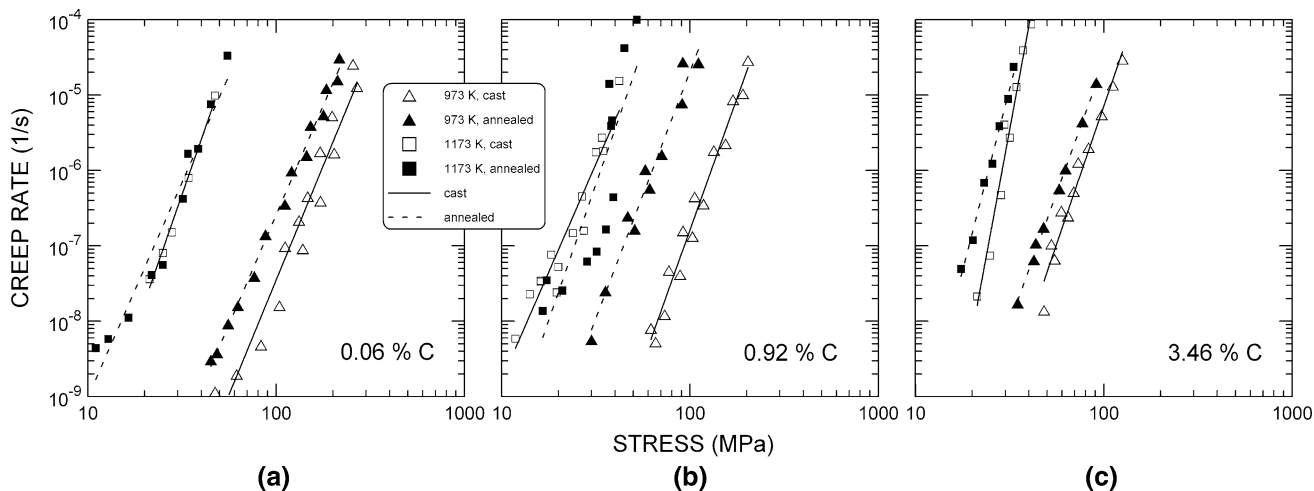


Fig. 7—Dependence of the creep rate on the applied stress separately for each tested alloy and heat-treatment history: (a) 0.06 at. pct C, (b) 0.92 at. pct C and (c) 3.46 at. pct C.

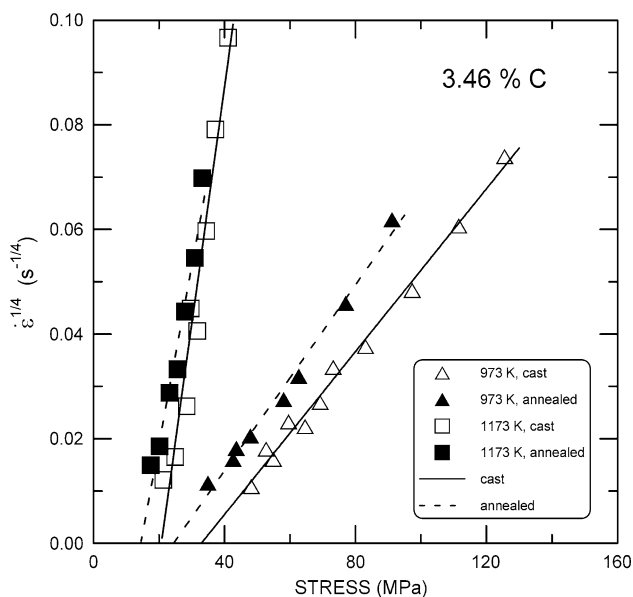


Fig. 8—Relation between $\dot{\epsilon}^{1/n'}$ and the applied stress for the true stress exponent $n' = 4$.

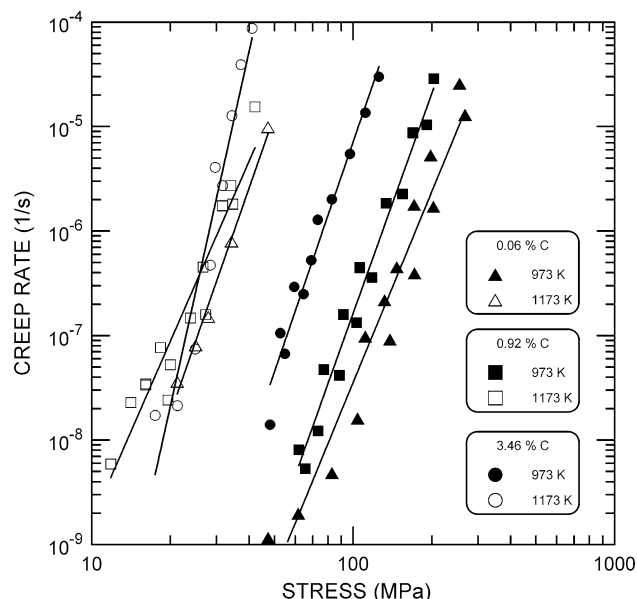


Fig. 9—Comparison of the effect of carbon content on the creep rate vs the applied stress dependence.

caution because the data are available for only two temperatures.

The values of stress exponent n in the two lower carbon alloys (Fe-25Al-5Zr and Fe-25Al-5Zr-1C) are similar to those usually observed in iron aluminides (cf. Table II in Reference 2). More specifically, the values correspond to those reported by McKamey *et al.*^[14] for Fe-28 Al-based alloys at higher stresses and suggest that the rate-controlling process is associated with dislocation climb.

Values of n are substantially greater in the high-carbon alloy (Fe-25Al-5Zr-4C) especially at the temperature of 1173 K (900 °C). The creep behavior can be rationalized by the threshold stress concept:^[39] the stress dependence of the creep rate is rewritten as

$$\dot{\epsilon} = A'(\sigma - \sigma_{th})^{n'}, \quad [2]$$

where A' is a temperature-dependent parameter and σ_{th} is the threshold stress. The value of n' should be close to the value of stress exponent n observed in pure metals and single-phase solid solutions. The value of the threshold stress can be determined by plotting $(\dot{\epsilon})^{1/n'}$ against the applied stress on linear axes for selected values of n' and extrapolating linearly to a zero creep rate. In accordance with the previous evaluations of the threshold stress in Fe-Al alloys with Zr additions,^[21,22] the same value of n' , *i.e.*, $n' = 4$, is used. The method is presented in Figure 8. The threshold stress equals 32.9 and 20.7 MPa at 973 K (700 °C) and 1173 K (900 °C), respectively, in the cast Fe-25Al-5Zr-4C alloy and 24.4 and 14.4 MPa at 973 K (700 °C) and 1173 K (900 °C), respectively, in the annealed Fe-25Al-5Zr-4C alloy. The temperature

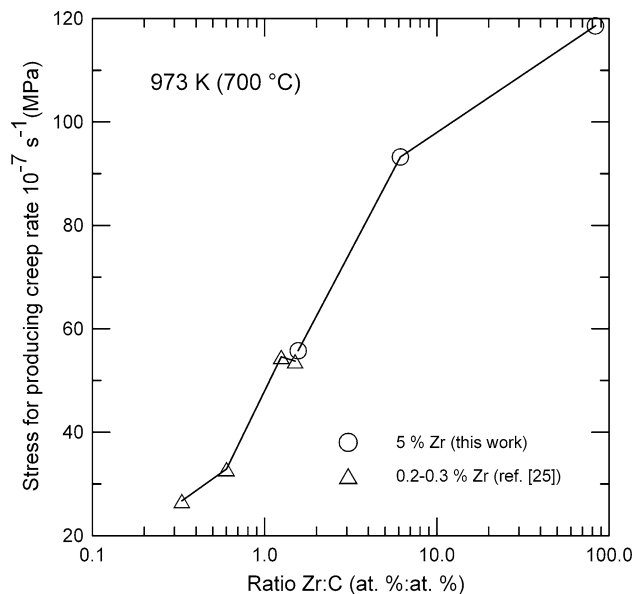


Fig. 10—The stress necessary to produce a creep rate of 10^{-7} s^{-1} as a function of $c(\text{Zr}):c(\text{C})$.

dependence of the estimated threshold stress is certainly stronger than that of the shear modulus. The threshold stress decreases due to annealing at 1273 K (1000 °C). This can correspond with the coagulation of precipitating phases. The threshold stress in the alloy Fe-25Al-5Zr-1C is probably much lower than the applied stresses in the creep experiments and cannot influence the value of the stress exponent n . The physical backgrounds of the threshold stress itself remain to be explained.

A comparison of the effect that the carbon additions have on the creep rate is given in Figure 9. The effect is small at 1173 K (900 °C), whereas the creep rate is increasing with the increasing carbon content at 973 K (700 °C), and the additions of carbon deteriorate the creep resistance of the Fe-25Al-5Zr alloy. In our previous work,^[25] the effect of combined C and Zr additives on the high-temperature mechanical properties was discussed in terms of the ratio of their concentrations: $c(\text{Zr}):c(\text{C})$. Here, we attempt to apply the same approach for the present alloys. In Figure 10, the stress for producing a creep rate of 10^{-7} s^{-1} is presented as a function of this ratio. It is clear that the present results coincide well with the previously published data. The effect of concentration for both additives is governed by the relations shown in the ternary Fe-Al-Zr phase diagram and its potential extension by adding carbon. The solubility of carbon in bcc Fe-Al alloys is not known exactly. In contrast to older investigations, a noticeable solubility up to 1.5 at. pct C was reported in Reference 36. This corresponds to the lowered amount of carbides observed after annealing in the alloy Fe-25Al-5Zr-1C. The excessive undissolved carbon in the Fe-25Al-5Zr-4C forms relatively great particles of ZrC that have only weak effect on the creep resistance. The presence of carbon reduces the amount of zirconium that is available for the formation of the Laves

phase and/or $\text{Fe}_{23}\text{Zr}_6$, and thus reduces the creep resistance.

V. CONCLUSIONS

In this work, compressive creep tests were conducted on Fe_3Al -based alloys with 5 pct zirconium and different carbon contents (0.06 to 3.46 pct). The results are summarized as follows:

- The values of the stress exponent in the low-carbon alloy are in the range of 6 to 7 and could be explained by the dislocation motion controlled by climb. The increased values of n in the high-carbon alloy at the temperature of 1173 K (900 °C) can be described by means of the threshold stress concept.
- Carbon additions deteriorate creep resistance at 973 K (700 °C). This result is discussed in terms of the ratio of zirconium to carbon in the alloy.
- An increase of the creep resistance with increasing ratio Zr:C is in agreement with the behavior observed previously in alloys with substantially lower concentrations of zirconium.

ACKNOWLEDGMENTS

The paper is based on work supported by the Czech Science Foundation within the Project 108/12/1452. J.V. and P.K. acknowledge support from the Project 16-05608S of the same foundation.

REFERENCES

1. G. Sauthoff: *Intermetallics*, VCH Verlagsgesellschaft, Weinheim, 1995, pp. 84–89.
2. N.S. Stoloff: *Mater. Sci. Eng. A*, 1998, vol. 258, pp. 1–14.
3. C.T. Liu, E.P. George, P.J. Maziasz, and J.H. Schneibel: *Mater. Sci. Eng. A*, 1998, vol. 258, pp. 84–98.
4. M. Yildirim, M.V. Akdeniz, and A.O. Mekhrabov: *Metall. Mater. Trans. A*, 2012, vol. 43A, pp. 1809–16.
5. D. Janda, H. Fietzek, M. Galetz, and M. Heilmaier: *Intermetallics*, 2013, vol. 41, pp. 51–57.
6. G. Yang and S. Milenkovic: *Intermetallics*, 2014, vol. 55, pp. 129–37.
7. X. Li, P. Prokopčáková, and M. Palm: *Mater. Sci. Eng. A*, 2014, vol. 611, pp. 234–41.
8. D. Janda, H. Ghassemi-Armaki, E. Bruder, M. Hockauf, M. Heilmaier, and K.S. Kumar: *Acta Mater.*, 2016, vol. 103, pp. 909–18.
9. M. Yildirim, M.V. Akdeniz, and A.O. Mekhrabov: *Mater. Sci. Eng. A*, 2016, vol. 664, pp. 17–25.
10. P. Prokopčáková, M. Švec, and M. Palm: *Int. J. Mater. Res.*, 2016, vol. 107, pp. 396–405.
11. L. Senčková, M. Palm, J. Pešička, and J. Veselý: *Intermetallics*, 2016, vol. 73, pp. 58–66.
12. M. Palm: *Intermetallics*, 2005, vol. 13, pp. 1286–95.
13. D.G. Morris and M.A. Muñoz-Morris: *Mater. Sci. Eng. A*, 2007, vol. 462, pp. 45–52.
14. C.G. McKamey, P.J. Maziasz, and J.W. Jones: *J. Mater. Res.*, 1992, vol. 7, pp. 2089–2106.
15. C.G. McKamey, P.J. Maziasz, G.M. Goodwin, and T. Zacharia: *Mater. Sci. Eng. A*, 1994, vol. 174, pp. 59–70.

16. C.G. McKamey and P.J. Maziasz: *Intermetallics*, 1998, vol. 6, pp. 303–14.
17. J.D. Whittenberger, M.V. Nathal, and D.J. Gaydos: *Intermetallics*, 1994, vol. 2, pp. 193–200.
18. T.M. Pollock, D.C. Lu, X. Shi, and K. Eow: *Mater. Sci. Eng. A*, 2001, vol. 317, pp. 241–48.
19. A. Wasilkowska, M. Bartsch, F. Stein, M. Palm, K. Sztwiertnia, G. Sauthoff, and U. Messerschmidt: *Mater. Sci. Eng. A*, 2004, vol. 380, pp. 9–19.
20. A. Wasilkowska, M. Bartsch, F. Stein, M. Palm, G. Sauthoff, and U. Messerschmidt: *Mater. Sci. Eng. A*, 2004, vol. 381, pp. 1–15.
21. D.G. Morris, M.A. Muñoz-Morris, and L.M. Requejo: *Acta Mater.*, 2006, vol. 54, pp. 2335–41.
22. D.G. Morris, I. Gutierrez-Urrutia, and M.A. Muñoz-Morris: *Scr. Mater.*, 2007, vol. 57, pp. 449–52.
23. J. Machida, S. Kobayashi, Y. Kaneno, and T. Takasugi: *Mater. Sci. Forum*, 2007, vols. 561–565, pp. 399–402.
24. M. Cieslar and M. Karlík: *Mater. Sci. Eng. A*, 2007, vol. 462, pp. 289–93.
25. P. Kratochvíl, F. Dobeš, J. Pešička, P. Málek, J. Buršík, V. Vodičková, and P. Hanus: *Mater. Sci. Eng. A*, 2012, vol. 548, pp. 175–82.
26. R.S. Sundar and S.C. Deevi: *Metall. Mater. Trans. A*, 2003, vol. 34A, pp. 2233–46.
27. P. Kejzlar, P. Kratochvíl, R. Král, and V. Vodičková: *Metall. Mater. Trans. A*, 2014, vol. 45A, pp. 335–42.
28. F. Stein, G. Sauthoff, and M. Palm: *Z. Metallkunde.*, 2004, vol. 95, pp. 469–85.
29. F. Stein and M. Palm: *Int. J. Mater. Res.*, 2007, vol. 98, pp. 580–88.
30. A.K. Mukherjee, J.E. Bird, and J.E. Dorn: *Trans. ASM*, 1969, vol. 62, pp. 155–79.
31. A. Lawley, J.A. Coll, and R.W. Cahn: *Trans. Metall. Soc. AIME*, 1960, vol. 218, pp. 166–76.
32. J.D. Whittenberger: *Mater. Sci. Eng.*, 1983, vol. 57, pp. 77–85.
33. J.D. Whittenberger: *Mater. Sci. Eng.*, 1986, vol. 77, pp. 103–13.
34. M. Eggersmann and H. Mehrer: *Philos. Mag. A*, 2000, vol. 80, pp. 1219–44.
35. L.N. Larikov, V.V. Geichenko V.M. Fal'chenko: *Diffusion Processes in Ordered Alloys*, Amerind Publishing Co., New Delhi, 1981.
36. M. Palm and G. Inden: *Intermetallics*, 1995, vol. 3, pp. 443–54.
37. W.D. Nix and B. Ilshner: in *Strength of Metals and Alloys*, P. Haasen, V. Gerold, and G. Kostorz, eds., Pergamon Press, Oxford, 1980, pp. 1503–30.
38. G. Antou, M. Gendre, E. Laborde, A. Maître, and G. Trolliard: *Mater. Sci. Eng. A*, 2014, vol. 612, pp. 326–34.
39. J.D. Whittenberger: *Metall. Trans. A*, 1977, vol. 8A, pp. 1155–63.